AUTHOR(S): DROUBI, M.G., FAISAL, N.H., ORR, F., STEEL, J.A. and EL-SHAIB, M.

TITLE: Acoustic emission method for defect detection and identification in carbon steel welded joints.

YEAR: 2017

Publisher citation: DROUBI, M.G., FAISAL, N.H., ORR, F., STEEL, J.A. and EL-SHAIB, M. 2017. Acoustic emission method for defect detection and identification in carbon steel welded joints. Journal of constructional steel research [online], 134, pages 28-37. Available from: https://doi.org/10.1016/j.jcsr.2017.03.012.

OpenAIR citation: DROUBI, M.G., FAISAL, N.H., ORR, F., STEEL, J.A. and EL-SHAIB, M. 2017. Acoustic emission method for defect detection and identification in carbon steel welded joints. Journal of constructional steel research, 134, pages 28-37. Held on OpenAIR [online]. Available from: https://openair.rgu.ac.uk.

Acoustic emission method for defect detection and identification in carbon steel welded joints

Mohamad G. Droubi[1], Nadimul H. Faisal[1], Fraser Orr[1], John A. Steel[1], Mohamed El-Shaib[2]

[1]School of Engineering, Robert Gordon University, Garthdee Road, Aberdeen, AB10 7GJ, UK

[2]Marine Engineering Department, Arab Academy for Science, Technology and Maritime Transportation, Alexandria, Egypt

Abstract

Detecting welding defects in industrial equipment (welded joints and built-up structures) is a key aspect in evaluating the probability of failure in different situations. Acoustic Emission (AE) is an effective non-destructive detecting technique, and can be a promising application for welding defect detection. This work presents a systematic experimental investigation on using AE technique for detecting and classifying different weld defects in carbon steel joint material. Four certified carbon steel samples were used in this study. A defect free control sample was used as the reference and three samples with induced defects, namely slag, porosity and crack. A pencil lead break (PLB) test was used to generate simulated AE sources on one side of the joint whereas the AE sensor was mounted on the other side to capture AE signals. A total of four experimental arrangements were used to investigate the effect of propagating distance (sensor to source distance) on the ability of AE to detect and identify defects in welds. For each of these arrangements, AE features such as peak amplitude, rise time, decay time, duration, and count numbers along with statistical features such as AE energy, root mean square (RMS) were extracted and analysed. Also, frequency analysis using FFT and wavelet transform were investigated for each weld test specimen for all arrangements. The results show that AE energy, peak amplitude and RMS

value can be used to automatically detect and identify the presence of a defect in carbon steel welds. It is concluded that AE has a considerable potential in use in welding inspection to assess the overall structural health and identify defects that can significantly reduce the strength and reliability of welded material and consequently reduce the risk of component's failure.

Keywords: Acoustic Emission (AE), welding inspection, defect detection.

1. Introduction

Welding inspection is an important practice to assess the integrity of any structure and its components in many industrial applications including pipeline systems in oil and gas, nuclear, power and petrochemical industries. Weld defects are generally divided into six types: porosity (PO), crack (CR), slag (SL), incomplete fusion (IF), incomplete penetration (IP) and no defect (ND). The presence of flaws in welded structures can be caused by a variety of reasons such as lamellar tearing which is often due to poor quality of steel, and cracking due to strain accompanying phase change and thermal shrinkage, as well as a wide variety of other reasons. Such flaws will indeed affect the structural integrity of welded structures, and as a result, welding requires regular inspection to monitor and assess their condition whether fit for a purpose or have lost part of their integrity due to aging problem and possibly take action when a defect is noticed before leading to leakages or failure. Therefore, detecting weld defects as early as possible is an essential step for the safety and continuity of operation of such structures.

Existing conventional non-destructive testing (NDT) techniques such as ultrasound testing (UT), eddy current (EC) and radiographic (especially X-ray technique) are the most commonly used techniques to inspect welding defects. Radiographic methods are based on the partial absorption of penetrating radiation as it passes through the object under

investigation. Nevertheless, a large number of radiographic images are analysed by inspectors which can lead to a subjective interpretation with the potential risk of overlooking defects. Eddy current testing is based on inducing electromagnetic currents in the object being inspected while observing the interaction between those currents and the object. Therefore, credible eddy current testing requires a high level of inspector training and awareness. Although ultrasonic testing has been widely used for the evaluation of welded joints, it is often very difficult to adequately perform the angle beam ultrasonic testing due to the presence of geometric reflectors such as weld roots and counter-bores which generate non-relevant signals. Even for more advanced ultrasonic techniques such as time of flight (TOF) or phased array (PA), such techniques can be inefficient as the interpretation and evaluation of inspection results depend on the operator's experience and knowledge. In this study, an acoustic emission (AE) measurement technique is investigated as an alternative non-intrusive method for inspection of welds. AE can be fast, repeatable and robust and offers very dynamic range and fidelity. Here, it is used for identifying three defects in butt-welded joints, being slag, porosity and crack, which are of growing interest in recent times.

Very limited work has been found in the literature that reports on using AE as a tool for welding inspection. Ranganayakulu *et al.* [1] utilized AE to study two weld defects, lack of penetration and lack of side fusion, in nuclear grade stainless steel materials. The results were analysed only in the time domain where energy, counts and amplitude of acquired AE signals were evaluated. They observed that both defects can be identified by using such different AE parameters where "counts vs. amplitude" parameter was found to give the widest distinction with respect to the type of defects. Aboali *et al*. [2] attempted to identify different types of welding defects using AE (generated from Pencil Lead Break (PLB) source) on butt welded carbon steel plates (Grade A36) of dimensions 300×300×10 mm, with three different types of weld defects namely; porosity, slag and lack of fusion. They observed

an increase in AE energy associated with slag defect compared to the other two welding defects. However, they were unable to discriminate between porosity and lack of fusion. Lee *et al.* [3] investigated the use of AE as a means for detecting weld defects in austenite stainless steel 316 material pipe. They induced an artificial crack of 20 mm length in the middle of the weld region while using laser guided wave as a non-contact method to simulating AE signals at one side of the pipe and attached AE sensor at the other side. For this very precise, repeatable source, comparing AE waveforms, frequency spectra and wavelet transforms with a free-defect specimen, they observed lots of wave modes and mode conversions due to the presence of the defect. Another study was conducted by Halim *et al.* [4] to detect and analyse different defects in ASTM A179 seamless steel tubes. They used an impact hammer to introduce AE signals. The features extracted from captured signals were compared between a healthy steel tube and four other tubes with different artificial defects. Using discrete wavelet transform on force and torque signals, Kumar *et al.* [5] investigated the detection of faults during friction stir welding on aluminium alloys of thickness 2.5 mm. They observed a sudden change in force signal with the presence of defect in welding. Finally, Yu *et al.* [6] investigated the use of AE to detect fatigue crack propagation in cruciform fillet welded joints. They found that AE absolute energy was the key factor in quantifying results in the time domain.

Detecting defects using AE is based on the interaction between a defect and elastic wave propagation (effect of defect) through the test samples where the characteristics of the observed signal will depend on the geometry and elastic properties of the target medium before being detected by a suitable AE sensor. Therefore, the aim of the present work is to develop a way in using AE as simple and reliable measure for weld health inspection and integrity assessment. This includes examining the capability of such technique in detecting the presence of a defect and discriminating the presence of different common types of defects

in weld test specimens which enable AE to contribute towards the improvement of the automatic detection and classification as well as an alternative screening tool for welding inspection.

2. Experimental procedure

2.1 Specimens

The essential experimental approach was to use a defect-free or no defect control specimen (ND) as a reference for characterizing acquired AE signal in the absence of a defect, then to carry out a comparative study with the other three-flawed weld specimens: crack (CR), slag (SL), and porosity (PO). The recorded AE features were examined to distinguish defective welds from the defect-free weld and also to see if it is possible to further identify and characterise each defect correctly based on results given by the generated AE signals. Therefore, four plates of 200 mm long, 100 mm wide and 10 mm thick made of carbon steel, a material that commonly used in structures, were used in this study. Such plates have single V-butt welds, on the middle of the upper surface, across the width, which is 100 mm long, 10 mm wide and 10 mm thick. All plates were supplied by Sonaspection Ltd, UK, which also introduced the artificial defects within the weld with a defect length being 25 mm and the tolerance on a defect length being ± 3 mm.

*2.2 AE **instrumentation and measurements***

In order to investigate the effect of sensor to source distance (propagating distance) on the ability of AE to detect and identify defects in welds, AE signals were acquired at different arrangements, as can be seen in **Figure 1(a)**, with distance between source and the sensor 100 mm, 75 mm, and 50 mm respectively. Four sets of experiments were carried out where the AE sensor (Micro 80D-93, Physical Acoustics Ltd., UK) was placed on the surface of the

target at its centreline and coupled by means of vacuum grease while pencil lead break (PLB) test was performed on the opposite side of the weld in an arrangement that the line between the source and the sensor passes through the centre of each welding defect. A pencil lead break test is a well-established procedure for generating simulated AE sources (Hsu-Neilsen source PLB [7]). Therefore, a commercial mechanical pencil with an in-house machined guide ring was used to generate simulated AE sources by breaking a 0.5 mm diameter and 2-3 mm length 2H pencil lead, as recommended by ASTM standards (E976-99) [7]. Also, to account for the effect of attaching and coupling the sensor onto the specimen, the AE sensor was installed and de-mounted 3 times at each arrangement with records of 10 pencil-lead breaks being acquired each time, so that 30 PLB were recorded for each arrangement. Then, the sensor was moved to the next arrangement, repeating the process for all four arrangements.

The AE data acquisition system is shown schematically in **Figure 1(b)** where the AE sensor is connected to a pre-amplifier offering a varied gain of (20/40/60 dB). The pre-amplifier was connected to an in-house-built 4-channel signal conditioning unit (SCU) that was coupled with a gain programmer in order to supply 28V of power, coupled with adjustable gain control. The SCU transmits the adjusted signal to a National Instruments (NI) BNC-2120 shielded connector block in order to complete the systems signal transmission to the data acquisition card (DAQ). The signals were interpreted through a computer using a 10 MS/s NI PCI-6115 DAQ in order to obtain the raw signal data and convert it to a binary file within the LabVIEW software for further analysis using MATLAB. The AE sensor, which was used for all experiments, was a commercially available “broadband” sensor of type Micro 80D-93, based on lead zirconate titanate (PZT). The sensor was 10 mm in diameter and 12 mm in length, and is not truly broadband but produces a relatively flat frequency response across the range (0.1 to 1 MHz) and operates in a temperature range of -65 to 177

C°. The pre-amplified data were acquired at 5 MHz for a record length of 20 ms. Silicone grease was applied to the sensor (to avoid any air gap) before attaching to the specimen surface using a magnetic sensor hold down clamp.

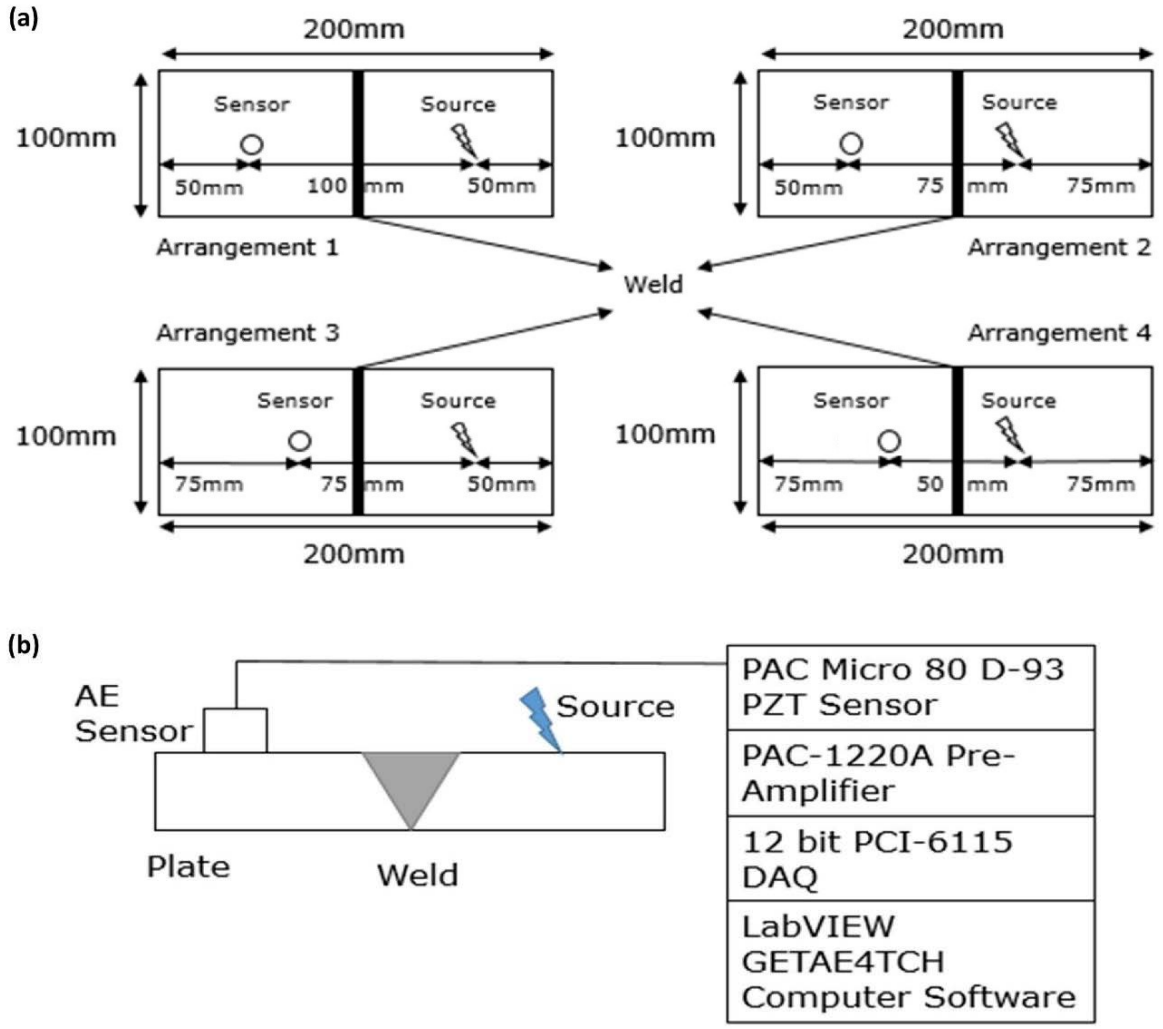

Figure 1. (a) Schematic layout for welding specimen showing each arrangement of AE sensor and PLB source, and (b) AE measurement system.

3. Results and discussion

The purpose of this work is to investigate whether or not an induced welding defect can be detected and classified using AE. Therefore, all observed AE signals have been analysed to extract their parameters in time, frequency and time-frequency domain. **Figure 2** shows typical raw AE signals for all work pieces (specimens) at arrangements 1 and 2,

respectively. As can be seen, the nature of acquired raw AE signal is complicated, by the defects being very similar across the record. Therefore, to identify different types of welding defects, AE signals were analyzed in dictating time and frequency processing approach.

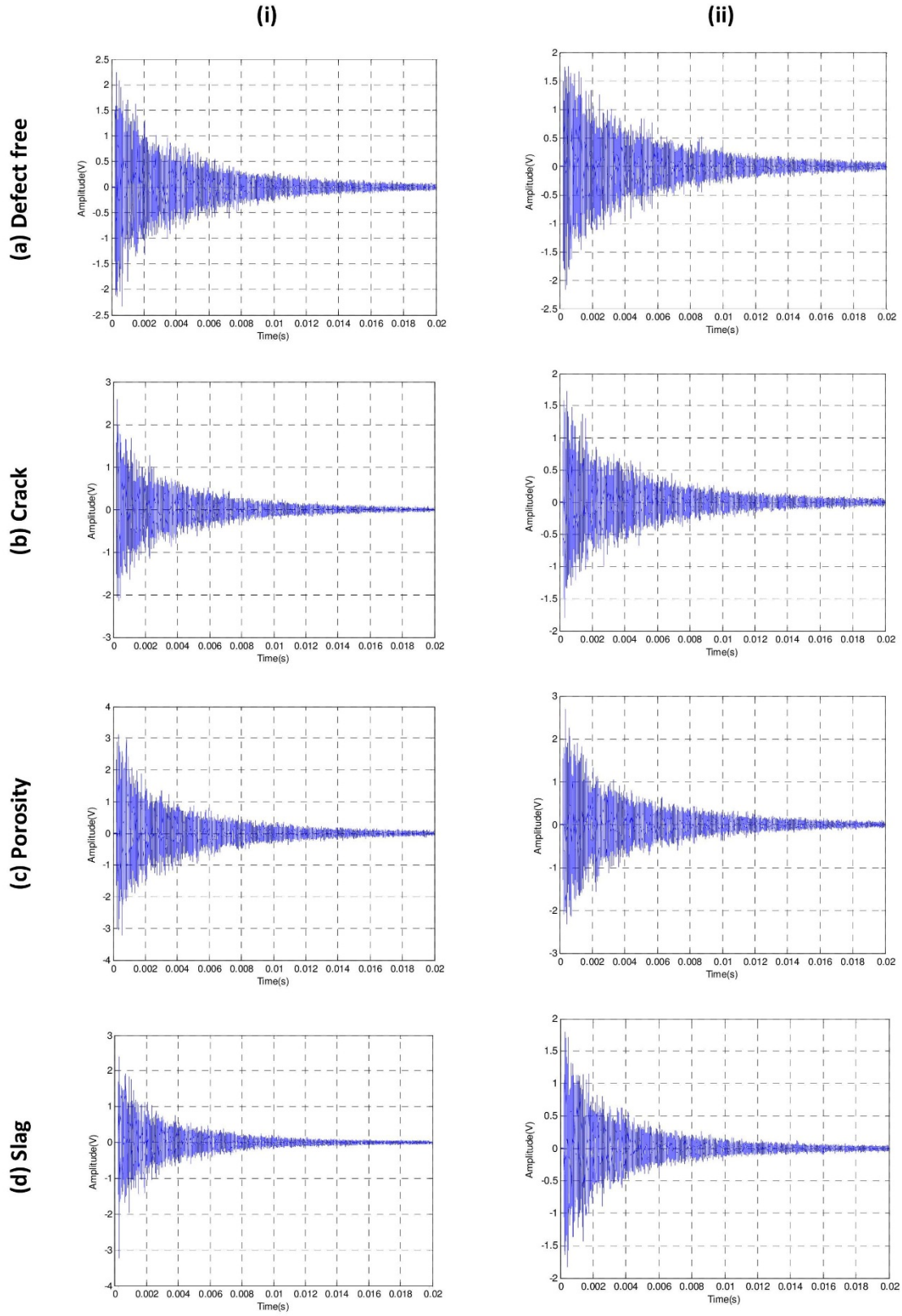

Figure 2. Typical 20 *ms* raw AE records for arrangements 1 and 2: (a) defect free, (b) crack, (c) porosity, and (d) slag.

3.1 Time domain signal analysis

The extracted AE parameters from each of the AE signals such as peak amplitude, counts, rise time, decay time and duration along with calculated AE energy and root mean square (RMS*)* were used in this study. At least thirty repeats (each 20 ms records) of PLB tests were analyzed for each arrangement and defect type, and the average value is used in the following analysis. To examine the capability of AE to detect the presence of a defect in weld test specimens and distinguish between defect types, the averaged values of AE parameters for all defective weld specimens were compared against the corresponding value of the defect free specimen (control). Then, the averaged values of defective specimens were compared to each other in an attempt to identify defect types.

As shown in **Figure 3**, time domain parameters for all tested specimens at each arrangements employed in this work are peak amplitude, rise and decay time, duration, counts, root mean square (RMS) and energy. Some of these features can be extracted directly from the captured AE signals such as amplitude, rise and decay time, duration and counts whilst RMS and energy are calculated from the AE events. The peak amplitude is maximum absolute value of an AE signal. The rise time is the time taken for the signal to first cross a pre-set threshold (i.e. 10% of peak amplitude) until the peak amplitude was reached whereas the decay time is the time taken for the signal to go from peak amplitude back to the threshold. The duration was the total time taken of the rise and decay times. Count is the number of times the acoustic emission signal exceeds the pre-set threshold within the event duration. The AE energy was calculated from the raw signal (measured as an amplified voltage, V) by integrating over the entire record: $E = \int_0^t V^2(t)dt$. Another statistical parameter which can be used as a measure of the energy of a signal is root mean square

(RMS) which can be expressed as: $RMS = \left(\frac{1}{n}\sum_{i=1}^{n} x_i^2\right)^{\frac{1}{2}}$; where, x_i is a set of n values {x_1, x_2,…, x_n} (or continuous-time waveform).

The peak amplitude for all AE signals associated with all test specimens at all arrangements is shown in **Figure 3(a)**. It is apparent that slag exhibited the highest peak amplitude values at all arrangements tested, which is in agreement with previous investigation [2]. It can also be seen that values at arrangement 1 are consistently greater than values at arrangement 2 indicating a reduction in peak amplitude as the source is moved nearer the sensor and weld. However, when the sensor is positioned closer to the weld (arrangements 3 and 4), it is clear that peak amplitude increases as the source-to-sensor distance decreases.

Figure 3(b) shows the recorded rise time for all weld test specimens at all arrangements tested where each column represents the average of thirty AE rise time values along with its standard deviation. Rise time is the time interval between the first threshold crossing, which was set to 10% of the maximum amplitude, and maximum amplitude of the signal. As can be seen, porosity has higher values than defect free while, in general, slag and crack have a lower value than the defect free. Overall, no trend can be observed between the defective welds compared to the reference weld with respect to the rise time.

Figure 3(c) shows the average decay time values for all samples at all arrangements tested. Generally, the decay time of each defective weld is lower than the reference weld except for porosity at arrangements 3 and 4. Decay time associated with slag and crack is consistently less than free in arrangements 1 to 3. A similar trend was obtained from **Figure 3(d)** which shows the average duration values for all samples at all arrangements tested. This is because the duration is the total time for rise and decay time.

It can be seen in **Figure 3(e)** that the number of counts of defective welds are very different from that of the reference weld in the first 3 arrangements, with defective welds

having a lower number of counts in all but one case (i.e. porosity at arrangement 3). It was found that as the sensor was brought closer to the weld (arrangements 3 and 4) porosity consistently had the highest number of counts. This can be confirmed by looking at the standard deviation values for each weld at arrangements 3 and 4. In general, slag and crack exhibited the lowest number of counts throughout each arrangement.

Figure 3(f) shows the recorded AE energy at all arrangements for all specimens. As can be seen, the test specimen with slag defect exhibits the highest average AE energy over other defective welds and free defect specimen at all arrangements, which is in agreement with previous observation [2]. This could be explained as some of the internal waves might reflect faster from the slag presence and convert to surface waves which have higher energy. The results follow a similar trend throughout with arrangement 4 always emitting the highest energy, followed by 3, then 1 and finally arrangement 2. This shows that the closer the AE sensor to the weld, the higher the energy emitted regardless of what type of weld was examined.

Figure 3(g) illustrates the variation of RMS for all defect types at all arrangements. The results acquired showed a similar tendency to **Figure 3(a)** but with less significant difference between crack and other weld test specimens fluctuates. As the sensor moves closer to the weld, the RMS values increase. Slag gave the highest values for each arrangement and crack gave the lowest values for each arrangement, perhaps making RMS relatively a good indicator of weld defects for these individual parameters. The porosity values, however, were extremely similar to the reference weld at each arrangement.

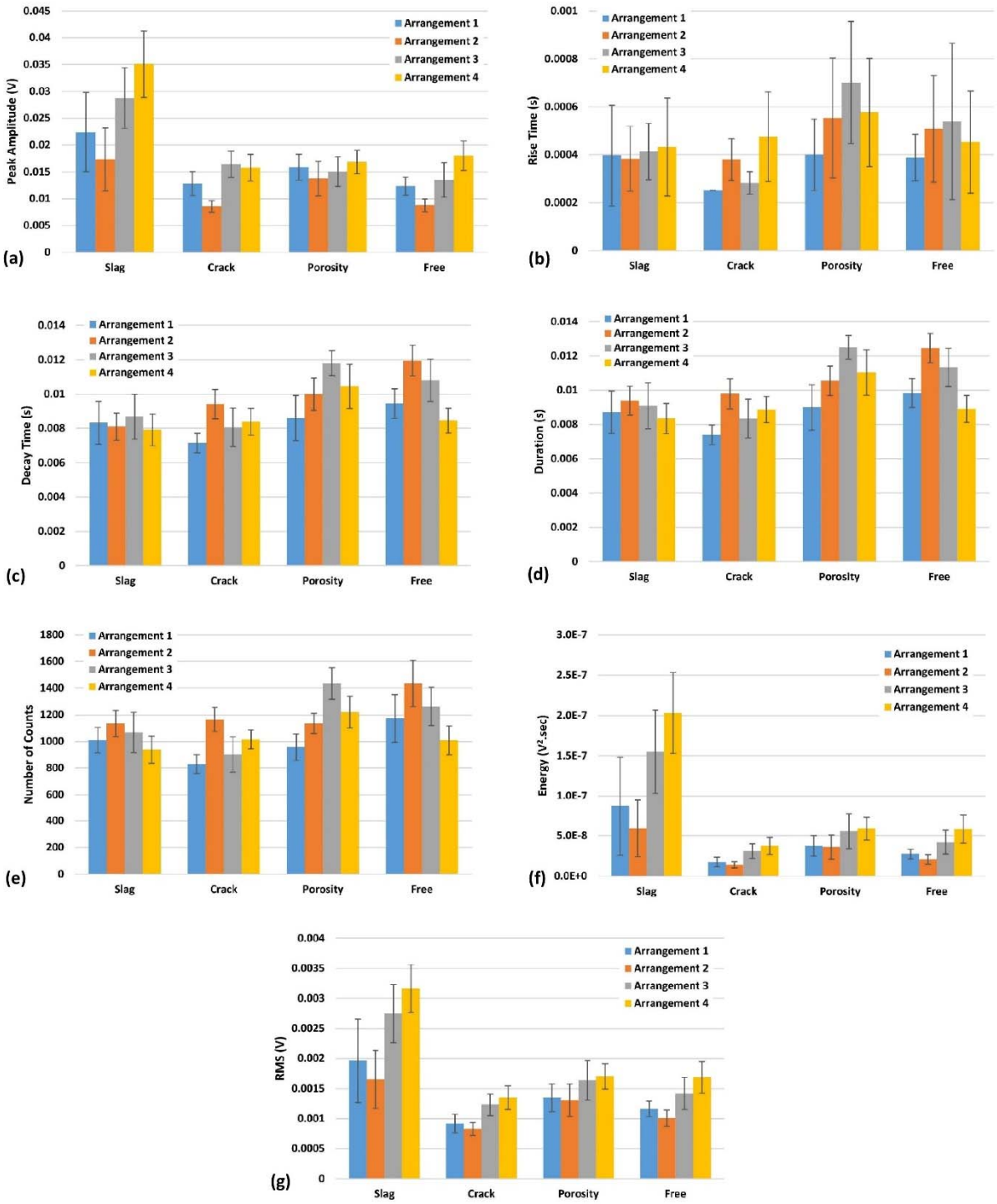

Figure 3. Time domain signal analysis for all tested weld specimens at each arrangement: (a) peak amplitude, (b) rise time, (c) decay time, (d) duration, (e) number of counts, (f) energy, and (g) RMS.

To develop an effective methodology for detection and identification of internal defects in V-butt welded samples, a percentage difference comparing each AE parameter for defective welds against the reference defect-free weld was devised. This percentage (%) difference was calculated by subtracting the value of the AE parameter of the reference weld (control specimen) from the defective weld and then dividing by the value of the reference weld. This value was then multiplied by 100 to give a percentage value:

$$\%difference = \frac{AE\ defective\ parameter\ value - AE\ reference\ parameter\ value}{AE\ reference\ parameter\ value} \times 100$$

Figure 4 show the percentage difference for each AE parameter at each arrangements (1, 2, 3 and 4). Again each column represents the average of 30 values along with their standard deviation. Arrangements 1 and 2 showed the same trend of percentage difference. AE Energy, maximum amplitude and RMS were found to be the 3 key parameters in identifying and detecting defects. Cracks were found to be the most difficult defect to characterise due to low percentage differences from the reference, whereas, slag and porosity values could be easily interpreted due to their differences in energy, maximum amplitude and RMS. In general, the differences appear to increase slightly as sensor to source distance decreases. As can be seen in **Figure 4(c)**, the recorded AE energy, amplitude and RMS contain the main distinguishable differences from each other for each defect types. Also, there were no significant difference between AE parameters for the porosity defect as they were in the previous two arrangements. **Figure 4(d)** shows the closest percentage difference between defects. Whilst the slag values for energy, amplitude and RMS remain similar to arrangement 3, the porosity and crack values tend towards 0% difference from the reference (control specimen) weld.

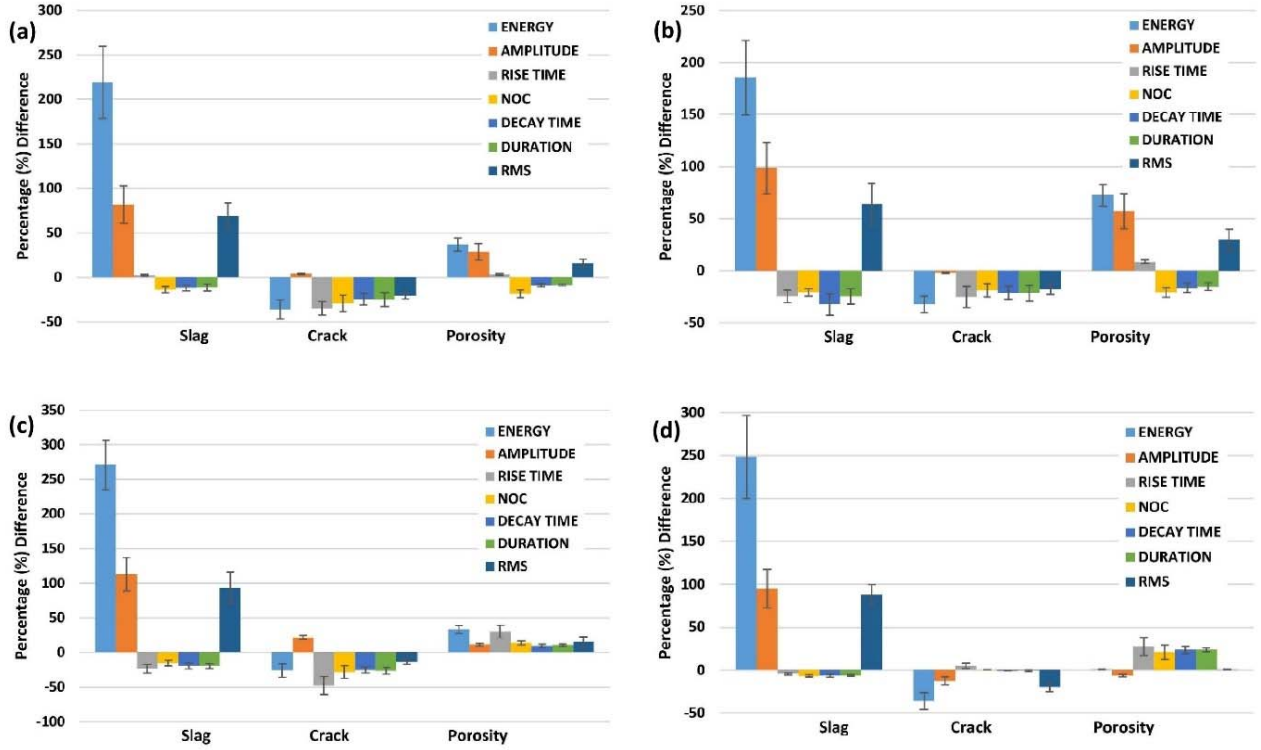

Figure 4. Percentage difference for each AE parameter in each defects at: (a) arrangement 1, (b) arrangement 2, (c) arrangement 3, and (d) arrangement 4.

3.2 Frequency domain signal analysis

Figure 5 shows examples of frequency spectra obtained for each weld test specimen at arrangement 1 and 2. The effect of the sensor bandwidth is apparent in the raw frequency spectrum, with most energy being contained in the range 100-400 kHz. The spectra show that most of the power is focused in three bands; one narrow band centred on a frequency of around 100 kHz, a band at 200 kHz to 300 kHz, and another band at 300 kHz to 400 kHz. It is also clear that, within its bandwidth, the sensor shows a systematic shift in frequency content (power) towards the higher end as the source to sensor distance decreases (arrangement 2).

In order to achieve greater level of comparison between the frequency spectrums obtained in **Figure 5**, a quantification method was devised in which the proportion of spectral

energy that is contained in each band was computed as $f_n = \frac{energy\ in\ \ band\ n}{total\ energy} \times 100\%$ (e.g. f_1 is the proportion of spectral energy contained in the frequency band 100-200 kHz), shown in **Figure 6**.

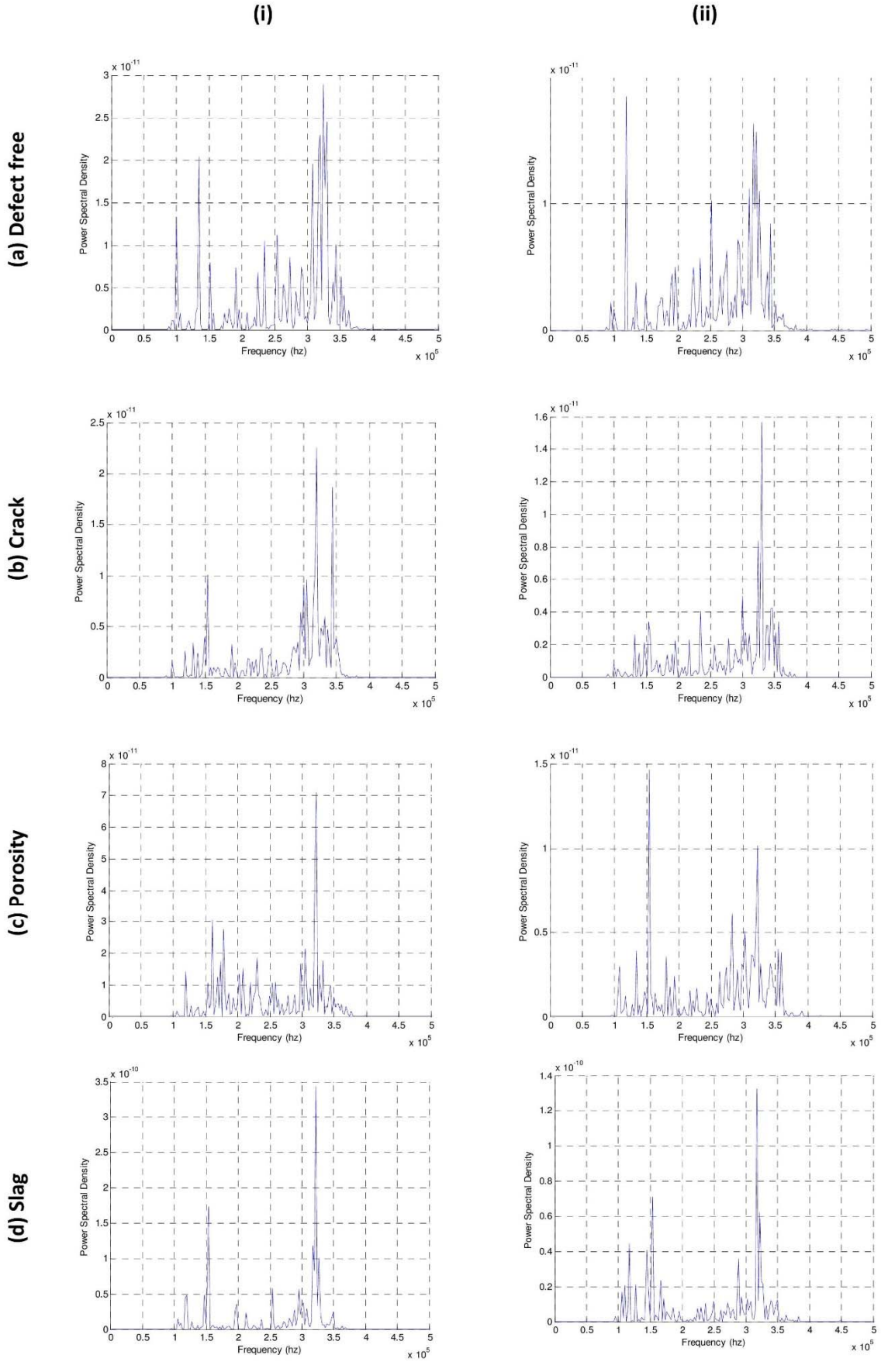
(i)
(ii)
(a) Defect free
(b) Crack
(c) Porosity
(d) Slag
Power Spectral Density
Frequency (hz)
x 10^-11
x 10^-10
x 10^5

Figure 5. Typical AE frequency spectra records for arrangements 1 and 2: (a) defect free, (b) crack, (c) porosity, and (d) slag.

Figure 6(a) shows the proportion of AE energy contained at each frequency band for all specimens at arrangement 1. It is clear that most of the spectral energy is contained in the frequency band f_3 (300-400 KHz). It can be seen that porosity defect could be distinguished from the other defects only at the highest frequency band. In general, the energy increasing as the frequency band increased, with the exception of porosity being smaller at f_2 than it was at f_1. It is worth mentioning here that both slag and crack defects could be distinguished from the no defect specimen, again, only at the highest frequency band f_3.

Similar trend was observed in **Figure 6(b)** which demonstrates the proportion of spectral AE energy associated with each frequency band for all welded specimens at arrangement 2. In general, the energy increasing as the frequency band increased, with the exception of porosity defect being smaller at f_2 than at f_1. It can be seen that slag and crack could be distinguished from the defect-free weld only at the highest frequency band f_3.

Figure 6(c) shows the energy proportion at arrangement 3. All specimens show increasing energy levels throughout the frequency bands apart from crack defect in band 2 having a lower energy than that of band 1. It is apparent that slag has the highest energy of the four specimens in f_3 and the lowest energy in f_1, making it easy to be distinguished. It was observed in f_2 that all values were fairly close and so characterisation of defects at this band in this arrangement was difficult. Also, the large difference between crack defect and no defect specimens at f_1 shows that cracks can be identified at this band fairly easily.

Finally, **Figure 6(d)** shows the proportion of spectral energy contained in each frequency band for all specimens at arrangement 4. As can be seen, slag defect again has the highest value at f_3 and lowest at f_1, making it distinguishable from other defects. Among all

specimens, porosity defects can be distinguished at f_2 and f_3 bands while crack defect can be distinguished at f_1 band. Among all defects, crack defect can be identified at f_1. This shows a good ability to detect and identify weld defects at arrangement 4 using the frequency domain method.

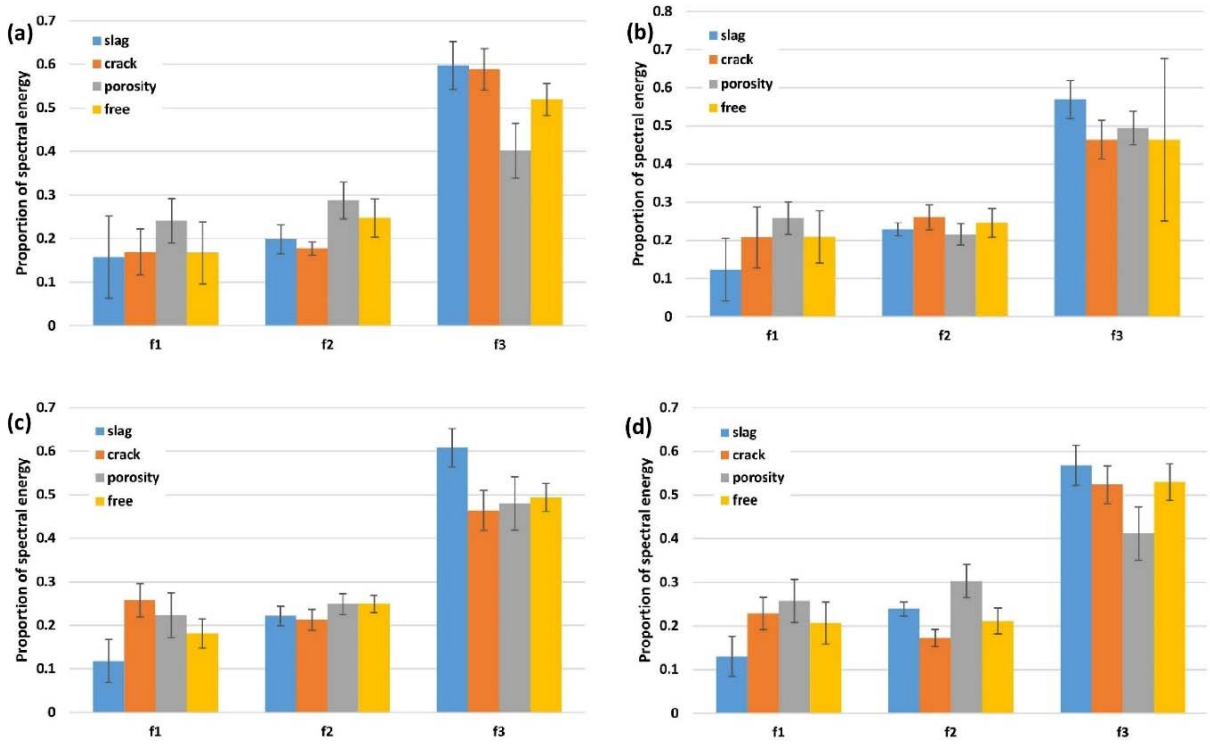

Figure 6. Proportion of spectral AE energy in raw frequency bands for all samples at: (a) arrangement 1, (b) arrangement 2, (c) arrangement 3, and (d) arrangement 4.

To summarise, slag could be easily detected when investigating different specimens as it shows the lowest spectral energy at bands f_1 and f_2, and the highest spectral energy at band f_3 in all arrangements tested in this study. Similarly, porosity defect was found most of the time (3 out of 4 arrangements) to show higher spectral energy than the no defect specimen at f_1 band. Also, porosity defect can be identified in f_3 band with values being lower than the no defect specimen in 3 out of the 4 arrangements. Moreover, the values are always significantly lower in f_3 band than the slag values, indicating that a difference between the

two defects can be identified easily. However, crack defect was fairly difficult to be identified from other defects as there was no distinguishable general trend in the results of the crack specimen but in 3 of the 4 arrangements, the crack defect value was lower than that of the no defect specimen and so could be detected as a defect.

3.3 Time-frequency domain analysis

Wavelet transform (WT) is a technique which represents any signal in the time-frequency domain. Most of the practical signals which exist are non-stationary, i.e. the frequency components present in the signal vary with time. Due to this, the existing techniques for analysing the signal in frequency domain such as Fourier Transform might be inappropriate as they only tell about the frequency components present in the signal and not about the localisation of those frequency components. Therefore, investigations in the time-frequency domain were carried out with wavelet analysis (AGU-Vallen Wavelet) which utilises a Gabor type wavelet. All signals were looked at over the first 500 μs and within a frequency band of the first 500 kHz due to this being the highest section of activity of the signal.

Typical AE waveforms for each weld specimen at arrangements 1, 2, 3 and 4 were chosen for analysis in order to show the effect of source to sensor distance. **Figure 7** shows the time-frequency plots for all weld specimens at arrangement 1 and 2. As can be seen, wavelets associated with different weld specimens are different in terms of intensity occurrence and frequency range. The results show that the maximum intensity of AE energy seems to appear at a frequency range between 250 kHz and 350 kHz but occur at different time which manifest the potential of using such technique in detecting and identifying weld defects. For instance, crack defect shows 3 areas of high and early intensity compared to one for porosity defect, whereas no high intensity was observed for slag defect.

Figure 8 illustrate a comparison between all weld specimen, but this time, for arrangement 3 and 4. It is clear that the frequency-time plots show higher output for each specimen with frequency as a function of time is more active for shorter source to sensor distance compared to **Figure 7.** These results suggest again the potential of using AE in weld inspection. For instance, in **Figure 8**, crack defect shows high intensity peaks after 250μs across two frequency ranges compared to porosity defect with frequency between 150μs and 250μs, whereas the maximum frequency for porosity defect occurs before 150μs. It is worth noting here that the closer the source to sensor distance, the more active the wavelet become.

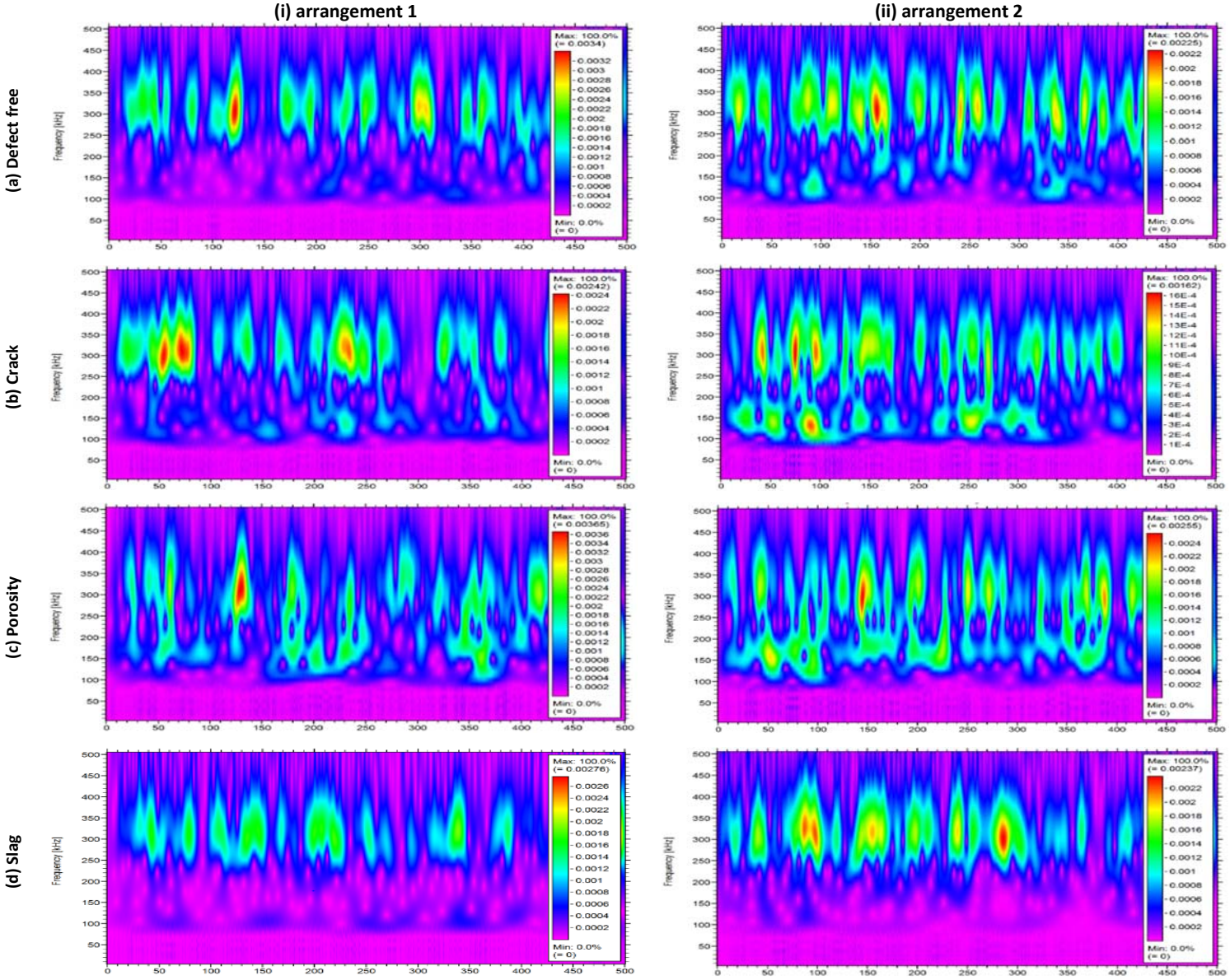

Figure 7. Wavelet analysis of AE signal records for arrangements 1 and 2: (a) defect free, (b) crack, (c) porosity, and (d) slag.

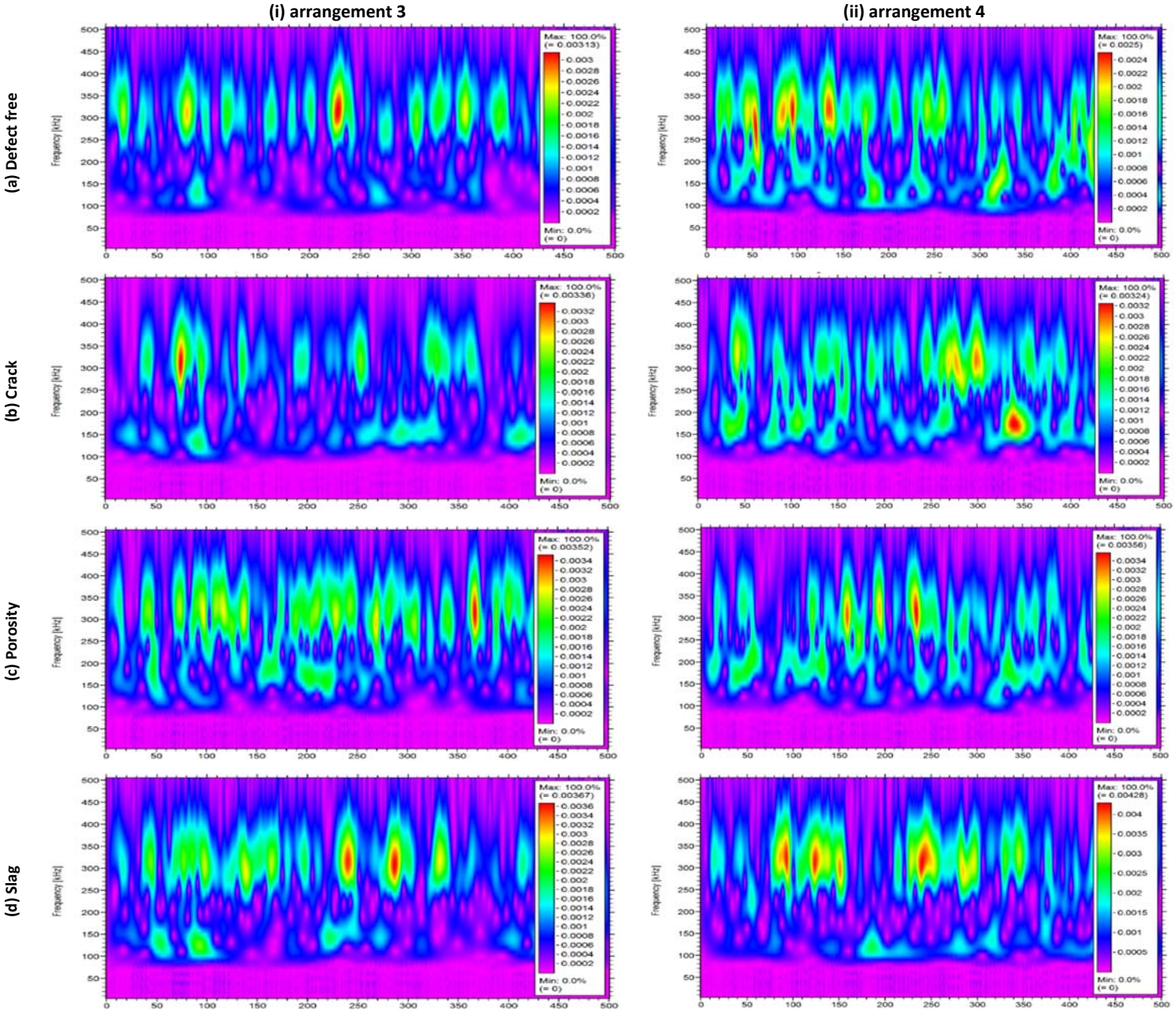

Figure 8. Wavelet analysis of AE signal records for arrangements 3 and 4: (a) defect free, (b) crack, (c) porosity, and (d) slag.

3.4 Future prospects

The key advantage that current AE method to analyse the welding defect offers, not available to other measurements, is the possibility to monitor the welded joint features (including defect and identification) with reasonable simplicity. It is clear that the uncertainty in quantifying the defect in welded joints makes other assessment of weld quality difficult for all but the simplest defect forms. It is therefore anticipated that correlation between AE parameters and weld defect types will lead to an improved method for welded joint quality evaluation. So far, the findings are limited to carbon steel material with a single defect in V-butt weld, and the following stages are required to bring the method to a point where it can be applied in real industrial welding inspection: (a) a set of experiments need to be carried out with different specimen materials to assess the extent to which the findings can be applied as material changes, making adjustments, as necessary; (b) another set of experiments need to be carried out to examine the potential of using AE technology in sizing different weld defects, and again to assess any adjustments that need to be made in the processing to use AE as a non- destructive diagnostic indicator for weld inspection.

Since the signal is restricted by the bandwidth of the AE sensor used, an empirical measurement of weld defects types makes it an appealing method of analysis. However, AE methods with the use of certain features (e.g. counts, energy, signal amplitude and its RMS, event duration, frequency spectrum, etc.) have some limitation in the characterisation of AE sources [8]. The appearance of multiple defects at different welded joint locations within the same specimen can superimposes the AE signals and signal reflections at edges and surfaces within the small or large structure test specimens. Therefore, an advanced signal processing characterisation methods are very much needed. By using AE signal patterns, identification of unknown signals and evaluating their significance, and correlating identified signals to the weld defect types, could further enhance quantitative interpretations of welded joint quality.

4. Conclusions

This work presents a systematic investigation into the application of AE technique in detection and identification of weld defects. In the presented paper, various types of welding defects have been evaluated using AE technique. The results of the investigation showed that AE parameters were influenced by defect presence, and hence, the findings from this experiment have shown evidence of the capability of AE technology to detect presence of different defects in V-butt welded specimens with the following broad conclusions:

a. AE offers the potential to detect and identify different weld defects and thus assess the overall structural health of welded structures.
b. Among all AE parameters tested in this study, AE energy, RMS and peak amplitude were found to be key parameters in detecting a presence of a weld defect. This was due to these three parameters showing the largest percentage differences from the no-defect values.
c. By analysing the proportion of AE energy contained in three frequency bands, frequency band 1 (100 kHz to 200 kHz) and frequency band 2 (300 kHz to 400 kHz) were found to be good indicators of detecting, and in some cases, identifying weld defects.
d. The wavelet transforms results were found overall to be able to accurately detect the presence of defective welds and also to identify the defect type. It was demonstrated that each defect could indeed be characterised and individually identified by looking at the energy intensity level and frequency range.
e. AE recorded by a sensor mounted on a weld specimen was strongly influenced by the distance between the source and the sensor.

References

[1] Ranganayakulu SV, Shiva Raju J, Kuchedludu A, Kumar, RB. Acoustic emission studies on weld bead defects in nuclear grade SS 316L materials. Open Journal of Acoustics 2014;4:115-130.

[2] Aboali, A, El-Shai M, Sharara A, Shehadeh, M. Screening for welding defects using acoustic emission technique. Advanced Materials Research 2014;1025-1026:7-12.

[3] Lee JK, Bae DS, Lee SP, Lee JH. Evaluation on defect in the weld of stainless steel materials using non-destructive technique. Fusion Engineering and Design 2014;89:1739-1745.

[4] Halim ZA, Jamaludin N, Junaidi S, Yahya SYS. Vibration impact acoustic emission technique for identification and analysis of defects in carbon steel tubes: Part B Cluster analysis. Journal of Mechanical Science and Technology 2015;29:1559-1570.

[5] Kumar U, Yadav I, Kumari S, Kumari K, Ranjan N, Kesharwani RK, Jain R, Kumar S, Pal S, Chakravarty D, Pal SK. Defect identification in friction stir welding using discrete wavelet analysis. Advances in Engineering Software 2015;85:43-50.

[6] Yu J, Ziehl P, Matta F, Pollock A. Acoustic emission detection of fatigue damage in cruciform welded joints. Journal of Constructional Steel Research 2013;86: 85-91.

[7] ASTM, 1999. E 976-99: Standard Guide for Determining the Reproducibility of Acoustic Emission Sensor Response.

[8] Faisal NH, Ahmed R, Reuben RL. Indentation testing and its acoustic emission response: applications and emerging trends. International Materials Reviews 2011;56(2):98-142.